Control Design of a De-Weighting Upper Limb Exoskeleton

Siti Khadijah Ali
Department of Multimedia
Faculty of Computer Science and Information Technology
Universiti Putra Malaysia
Serdang, Malaysia
*ctkhadijah@upm.edu.my

M. Osman Tokhi
Department of Electrical and Electronics Engineering
London South Bank University
London, United Kingdom
tokhim@lsbu.ac.uk

***Abstract*—One of the most common problems in humans is a muscle fatigue. Exoskeletons are known as one of the solution to deal with human muscle fatigue. However, several issues related to the development of exoskeletons for such a case have been identified. One of these is the control mechanism. Thus, the objective of this paper is to investigate development of a control strategy for the upper-limb exoskeleton. In this paper, a new control mechanism for an upper-limb exoskeleton is proposed. A fuzzy-based PD controller and PID are used in the proposed control mechanism, and a comparative assessment of the performance of both controllers is made. The results show that the control mechanism with fuzzy-based PD controller performs better than the PID controller in terms of trajectory tracking accuracy and control torque analysis.**

***Index Terms*—Exoskeleton, Kinematics and dynamics, Euler-Lagrange approach, Fuzzy-based control**

I. Introduction

Muscle fatigue is a natural phenomenon that occurs due to inability of muscle to exert force in response to a voluntary effort. It could cause the reduction of power, lead to discomfort and pain. In addition, muscle fatigue could lead to musculuskeletal disorder (MSD) and cumulative trauma disorder (CDT) [1]–[5].

Several types of fatigue models are developed to avoid the associated health problems in the working population such as [6], [7], [8], [9], [10] and [11]. In general, most of the developed fatigue models are used to identify the occurrence of fatigue and to reduce the MSDs by identifying suitable postures during work. These models are used in ergonomics research for indutrial applications. Another technique to reduce the fatigue, is by supporting human with an exoskeleton. Several works have been done to investigate the capability of the exoskeletons in supporting and helping human in performing tasks.

Exoskeletons could be categorised based on the application, human-interaction, mechanical design and control approach. In terms of application, exoskeleton has been developed to provide support to patients during rehabilitation [12]–[14]. Exoskeletons have also been developed for assisting people with a limited range of arm movements during activities of daily living (ADL) [15]–[17]. Further developments of exoskeletons have been for augmentation of physical capability of healthy people while carrying physical tasks [18], [19].

During the development of the exoskeleton, it is essential to ensure that the control startegy is effective, so that the exoskeleton could be operated harmoniously with the human upper-extremity. Therefore, the control mechanism for an upper-limb exoskeleton is proposed.

II. Methodology

A. System Description

SolidWorks is used to model a humanoid and to design the upper-extremity exoskeleton (Figure 1), as it allows to design complex 3D realistic models. In addition, the designs can easily be imported to other software/applications such as VisualNastran and Simmechanics.

Fig. 1: The exoskeleton is attached parallel to human

The humanoid is developed to represent the human-like physical system in terms of measuments of mass, height and length (Figure 1(a)). The measurements for the length and mass of human model are taken from [12] (Table I).

The design of an exoskeleton used in this work is inspired by TitanArm [20]. This design is chosen because it is simple, capable of powered use and data transmission in a mobile fashion. The exoskeleton was designed with aluminum to provide the exoskeleton structure with a relatively light weight, since aluminum is a low density material and has reasonable

TABLE I: Physical model parameters

Segment	Length (cm)	Weight (kg)
Head	22	3
Neck	8.8	1.085
Trunk	49	34
Pelvis	5	4.686
Upper Arm	31.32	2.17
Lower Arm	28.08	1.30
Hand	19.42	0.49
Thigh	41.6	7
Calf	41.8	3.26
Foot	25.8	1.015

strength characteristics. The exoskeleton is designed to be worn on the lateral side of the upper limb in order to provide naturalistic movements of the shoulder, elbow and wrist joint (Figure 1). The designed exoskeleton has four revolute joints. The human-exoskeleton design, is then imported to Simmechanics for control system evaluation purpose.

B. Kinematics of the designed exoskeleton

Kinematics and dynamics are the two terms mostly used in robotic research. Kinematics is defined as the study of motion without considering the force, torque and moment. Two groups of kinematics are, forward kinematics and inverse kinematics. Forward kinematics is a process of obtaining the end-effector position when the angles of the joints are given. Inverse kinematics is a process of calculating the angles of the joints when the end-effector position is given. This may be described as in Figure 2.

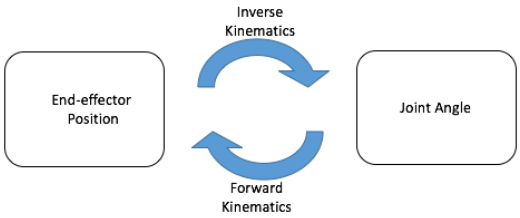

Fig. 2: Forward and Inverse Kinematics

1) Forward Kinematic: The Denavit-Hartenberg (DH) convention is used to obtain forward kinematics. The DH notation is chosen because it allows composing coordinate transformation into one homogenous transformation matrix. The homogenous transformation matrix provides the relative position and orientation of two consecutive frames. This information is used to connect two consecutive frames. The two consecutive frames could be described as $i-1$ and i. As shown in Figure 3 (a), the base frame for the exoskeleton is denoted as O_0. The O_0 also represents the shoulder adduction/abduction motion. The O_1, O_2 and O_3 represent shoulder internal/external motion, shoulder extension/flexion and elbow extension/flexion respectively. O_4 represents the end-point of the exoskeleton.

In Figure 3 (b), the DH table consists of four parameters : θ_i, α_i, a_i and d_i where i

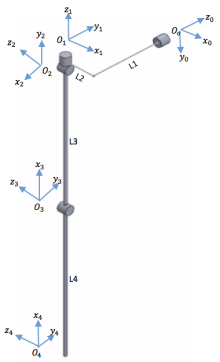

(a)

Frame	θ_i	α_i	d_i	a_i
1	θ_1	$\frac{\pi}{2}$	L_1	L_2
2	$\theta_2 - \frac{\pi}{2}$	$\frac{\pi}{2}$	0	0
3	$\theta_3 + \frac{\pi}{2}$	0	0	L_3
4	θ_4	0	0	L_4

(b)

Fig. 3: (a) Schematic Diagram (b) Denavit-Hartenberg Table

1) θ_i represents the angle between X_{i-1} and x_i measured around Z_{i-1}
2) α_i represents the angle between Z_{i-1} and Z_i measured around X_i
3) a_i is the distance along X_i from O_i to the intersection of the axis X_i and Z_{i-1}
4) d_i is the distance along Z_{i-1} from O_{i-1} to the intersection of X_i and Z_{i-1} axes

There are steps to determine the frame for each joint. The first step is to determine the origin of the axes, denoted by O_i. The z-axis designates the direction of motion for each joint. The O_1, O_2, O_3 and the z-axes for the designed exoskeleton are shown as in Figure 3. The following step is to determine the x-axes for the joints. There are three rules to choose the direction of the x-axis. The rules are based on the position of the Z_{i-1} and Z_i, and are given as follows:

(i)

1) If the Z_{i-1} and Z_i are not co-planar, there exists a unique line segment perpendicular to both Z_{i-1} and Z_i. This line defines x-axis for frame i.
2) If the Z_{i-1} and Z_i are parallel, there exists an infinite line segment perpendicular to Z_{i-1} and Z_i, and the x-axis for frame i can be chosen from one of these lines. There are two options for choosing the direction of the x_i-axis ; could be pointing to Z_{i-1} and not pointing to Z_{i-1}. For this category, the d_i and a_i, both will be equal to 0.
3) If the Z_{i-1} and Z_i are intersecting, the X_i is chosen normal to the plane formed by Z_{i-1} and Z_i. For this case, the a_i would be equal to 0. The final step is the assignment of the y-axes. The y-axis is gathered using the right-hand rule.

In the next section, the control mechanism of an upper-limb exoskeleton is presented.

III. Control Mechanism of an Upper-limb Exoskeleton

The control strategy of the exoskeleton is shown in Figure 4. The controller starts with the identification of the source

of reference trajectory. The reference or the desired trajectory could be obtained in two ways; from a predefined trajectory or gathered from a human. Since the focus of the paper is to investigate the possibility of the control design in controlling the exoskeleton, a predefined trajectory is used. The predefined trajectory is obtained from [23].

The exoskeleton consists of four joints which represent the shoulder abduction/adduction (J1), shoulder internal/external (J2), shoulder flexion/extension (J3) and elbow flexion/extension (J4). Joint activation will identify which joint is moving at one time. The joint activation is needed to ensure that the movement of the exoskeleton joint is parallel to human progress. To activate the joint movement, three pieces of information are needed. These are the current desired trajectory, the previous desired trajectory and the reference selection. Three important questions need to be asked before applying conditions to activate the joints;

1) How is the reference is obtained?
2) How to identify that the joint is moving?
3) What is the direction of the movement?

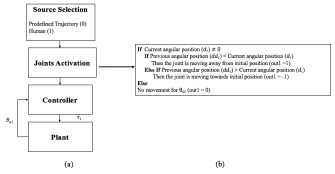

Fig. 4: Control design: (a) Control structure of an exoskeleton (b) The process of joints activation

The first question is answered by the selection of the reference. In this paper, the predefined trajectory is used. Hence the 'Ref' is equal to '0' (Figure 4 (b)). For the second question, to identify that the joint is moving, a condition is applied. The current desired trajectory (θ_{di}) is tested. If $\theta_{di} \neq 0$, where $i = 1, 2, 3, 4$, then, the joint is moving. For the third question, two types of direction are identified. The joint could move approaching or move away from the initial position of the exoskeleton. To identify this, the current desired trajectory (θ_{di}) and previous desired trajectory (θ_{ddi}) are compared. The joint is moving away from the neutral position if $\theta_{ddi} < \theta_{di}$ and the joint is approaching the neutral position if $\theta_{ddi} > \theta_{di}$.

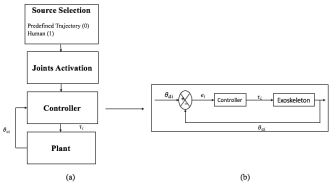

Fig. 5: Control design: (a) Control structure of an exoskeleton (b) Controller

There are three possible outcomes (out_i) from these conditions, and they are identified as 0, -1 or 1. The $out_i = 0$ means no movement for the joint. If $out_i = 1$, the joint is moving away from the neutral position of the exoskeleton. If $out_i = -1$, the joint is approaching the neutral position of the exoskeleton. If $out_i = 1$ or $out_i = -1$, then, the current desired trajectory (θ_{di}), is sent as the desired trajectory of the exoskeleton. The process in 'Joints Activation' has been summarised in Figure 4 (b).

The out_i will let the system know which joint needs to be moved. Then, the error is measured between the current desired trajectory (θ_{di}) and the actual trajectory, and then the error is sent to the controller. Based on the error information, the controller generates an appropriate amount of torque to produce the desired position of the joint. Figure 5 (b) shows the feedback control system of the exoskeleton.

To ensure that the power consumption is less, the combination of fuzzy-based Proportional Derivative (PD) is chosen. This is due to the ability of PD in minimizing the steady-state error and the rise time. Whereas, Proportional-Integral-Derivative (PID) controller was used as a baseline for comparison purpose.

A. Implementation of the controllers

Figures 6 and 7 show the implementation of the PID and fuzzy-based PD controllers on the exoskeleton for each joint in a joint-space environment.

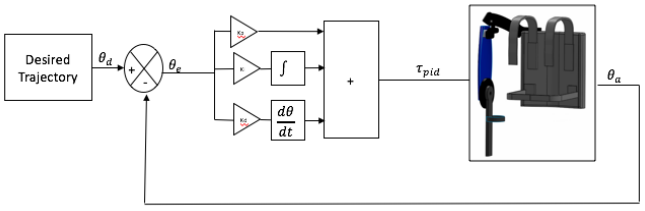

Fig. 6: Block diagram of the PID controller

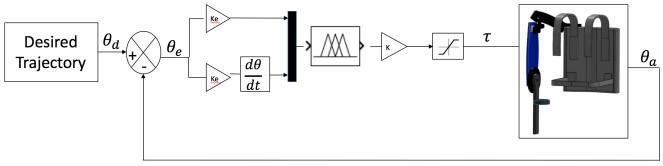

Fig. 7: Block diagram of the fuzzy-based PD controller

The input to the PID controller is the tracking error (θ_e). The tracking error is obtained by subtracting the desired trajectory from the actual trajectory of the exoskeleton. The input to the fuzzy-based PD are the tracking error (θ_e) and the rate of the change of the tracking error ($\dot{e}$). Then, based on the inputs, both controllers generate the control signal. The control signal is fed to the exoskeleton. The actual trajectory from the exoskeleton is fed back and compared to the desired trajectory. This process will continously occur until the desired trajectory is achieved.

In developing the fuzzy-based PD controller, the Gaussian type membership (MFs) is chosen to ensure the system response is smooth. The five MFs are Negative Big (NB), Negative Small (NS), Zero (Z), Positive Small (PS) and Positive Big (PB). These membership functions were normalised in the range of [-1, 1]. It is known that the inputs (b) are two, and the membership functions (m), are five. Hence, using the formula m^b, the number of rules are $5^2 = 25$ for each fuzzy controller with 50 $\%$ overlap between MFs. The 25 rules are presented in Table II and the details are presented in Figure 8.

TABLE II: Construction of fuzzy rules

$e/\dot{e}$	NB	NS	Z	PS	PB
NB	PB	PB	PB	PS	Z
NS	PB	PB	PS	Z	NS
Z	PB	PS	Z	NS	NB
PS	PS	Z	NS	NB	NB
PB	Z	NS	NB	NB	NB

In general, if error and change of error are both positive big (PB), the control action will produce negative big (NB) signal to bring back the output to the desired trajectory. On the contrary, if error and change of error are both negative big (NB), the control action will supply the positive big (PB) signal to ensure the output trajectory goes to the desired position. In case the error is positive big (PB) and change of error is negative big (NB) or vice-versa, zero (Z) control signal is applied to the system as the system will be in a steady-state condition.

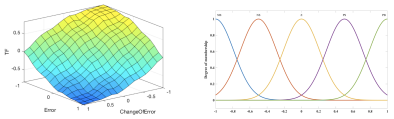

Fig. 8: Details of fuzzy-based PD control: (a) Fuzzy logic 3D surface (b) Membership functions for inputs and outputs for the exoskeleton joints motions

These rules are developed based on the knowledge to minimize the position error of each joint of the exoskeleton and to ensure the smoothness of the motion. In addition, the max-min inference is used to ensure that the exoskeleton could be moved fast. The centroid or centre of gravity is chosen to be used during the defuzzification process due to its fine and smooth transition output.

The performance of tracking desired trajectory, deviation or error of trajectory and torque needed for moving the joints of both controllers are presented in the next section.

IV. Results and Discussion

In this section, the results and discussions on the performance of PID and fuzzy-based PD controller are presented. The trajectory tracking and error performance, and torque required by the PID and fuzzy-based PD are presented. This section begins with results of PID, and follows with fuzzy-based PD controllers.

To observe both controllers, two joints were active (Joint 1 and Joint n4) while the remaining joints were passive. The desired trajectory for all joints is shown in Figure 9.

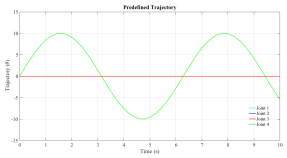

Fig. 9: Predefined trajectory

The gains for PID and fuzzy-based PD were tuned using a heuristic approach and these are shown in Tables III and IV.

Figure 10 shows the results of PID controller for trajectory tracking, deviation of motion and the torque required for all joints. In general, all joints were able to track the desired trajectory.To compare the error performance, Root Mean Square Error (RMSE) and Maximum Absolute Error (MAE) were used. In addition, to evaluate the torque performance, the Maximum Absolute Torque (MAT) was used. The measurements of RMSE, MARE and MAT are presented as:

$$RMSE = \sqrt{\frac{\sum_1^n (\hat{\theta} - \theta)^2}{n}} \tag{1}$$

$$MAE = max(|\hat{\theta} - \theta|) \tag{2}$$

$$MAT = max(|\tau|) \tag{3}$$

where $\hat{\theta}$ is the desired position and θ is the actual position; n is the number of data.

The RMSE of PID controller for Joint 1, Joint 2, Joint 3 and Joint 4 were 0.0814°, 0.0056°, 0.0695° and 0.0680°. The MAE of Joint 1, Joint 2, Joint 3 and Joint 4 were 0.2455°, 0.01174°, 0.1036° and 0.111°. The MAT for PID were 3.154 Nm, 0.1169 Nm, 0.8769 Nm and 0.944 Nm for each joint of the exoskeleton.

TABLE III: PID controller gains

Gains	Joint 1	Joint 2	Joint 3	Joint 4
K_P	10	1.0	1.0	1.0
K_I	5.5	0.5	0.5	0.5
K_D	0.3	0.5	0.5	0.1

Figure 11 shows the trajectory tracking, deviation (error) and torque required for the fuzzy-based PD controller. In general, each joint was able to follow the desired tracjectory. Spikes occurred at each joint at $t = 0$ was considered small and could be neglected. In addition, usually, any jerk that occurred in the beginning of the movement could be ignored because the system needed some time at start to stabilise.

Table VI shows the comparison values of the RMSE, MAE and MAT for the PID and fuzzy-based PD controller. In terms of deviation analysis, it shows that the RMSE and MAE of the fuzzy-based PD controller is less compared to PID. However,

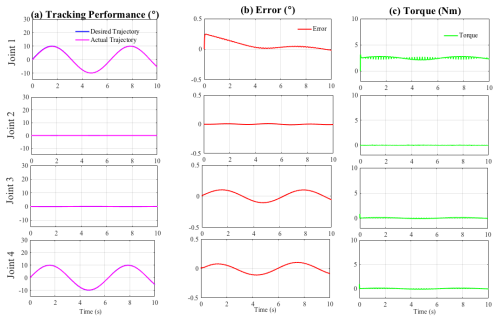

Fig. 10: Performance of PID controller: (a) Trajectory tracking (b) Error (c) Torque

TABLE IV: Fuzzy-based PD controller gains

Gains	Joint 1	Joint 2	Joint 3	Joint 4
K_e	1	0.5	0.5	0.5
$K_{\dot{e}}$	0.002	0.05	20E-04	2E-04
K	250	100	100	100

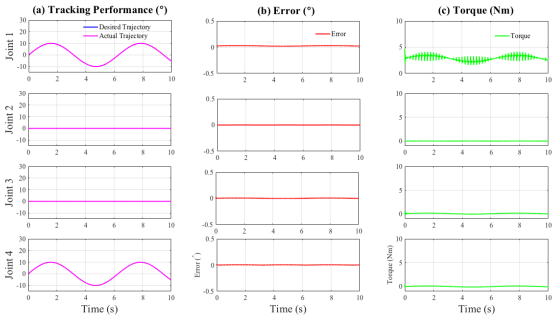

Fig. 11: Performance of fuzzy-based PD controller: (a) Trajectory tracking (b) Error (c) Torque

the MAT of Joint 1 for fuzzy-based PD is higher about 30% than PID. However, the MAT value for fuzzy-based PD is in an acceptable range (Table V).

TABLE V: Torque limits of human arm ([12], [21], [22])

Joint	Human strength (Nm)
Shoulder flexion/extension	115/110
Shoulder abduction/adduction	134/94
Elbow flexion/extension	72.5/42
Forearm pronation/supination	9.1/7
Wrist palmer/dorsal flexion	19.8
Wrist abduction/adduction	20.8

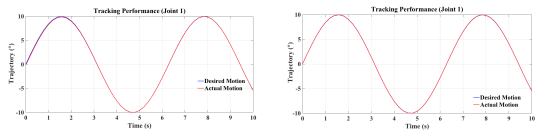

(a) (b)

Fig. 12: Trajectory tracking performance of (Joint 1): (a) PID (b) Fuzzy-based PD controller.

TABLE VI: RMSE, MAE and MAT for PID and fuzzy-based PD controller

Joint/Movement	RMSE		MAE	
	PID	PD-Fuzzy	PID	PD-Fuzzy
Joint 1	0.0814	0.02528	0.2455	0.03348
Joint 2	0.0056	0.00005090	0.01174	0.0009336
Joint 3	0.0695	0.005941	0.1036	0.0114
Joint 4	0.0680	0.003584	0.111	0.01883

Joint/Movement	MAT	
	PID	PD-Fuzzy
Joint 1	3.154	4.122
Joint 2	0.1169	0.04840
Joint 3	0.8769	0.1322
Joint 4	0.944	0.1484

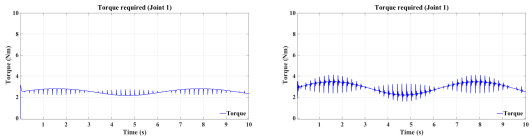

(a) (b)

Fig. 13: The torque required by (Joint 1): (a) PID (b) Fuzzy-based PD controller.

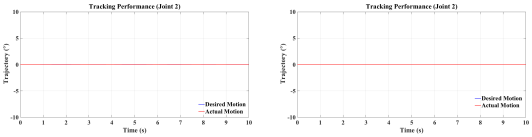

(a) (b)

Fig. 14: Trajectory tracking performance at Joint 2: (a) PID (b) Fuzzy-based PD controller.

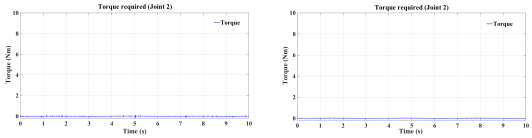

(a) (b)

Fig. 15: The torque required by Joint 2: (a) PID (b) Fuzzy-based PD controller.

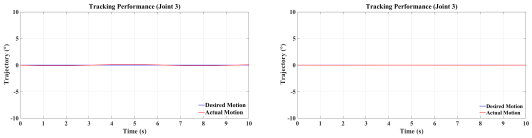

(a) (b)

Fig. 16: Trajectory tracking performance at Joint 3: (a) PID (b) Fuzzy-based PD controller.

Figure 12, Figure 14, Figure 16 and Figure 18 show tracking performances of system with PID and fuzzy-based PD controller. Figure 13, Figure 15, Figure 17 and Figure 19 show comparative results in terms of torque required by the

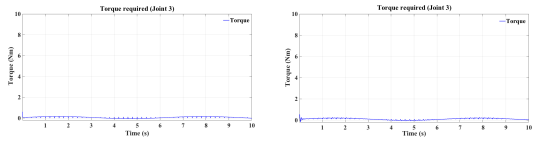

(a) (b)

Fig. 17: The torque required by (Joint 3): (a) PID (b) Fuzzy-based PD controller.

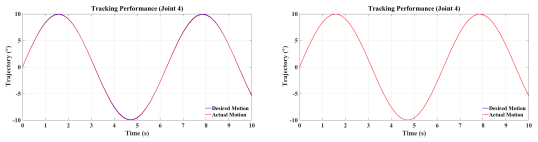

(a) (b)

Fig. 18: Trajectory trajectory performance at Joint 4: (a) PID (b) Fuzzy-based PD controller.

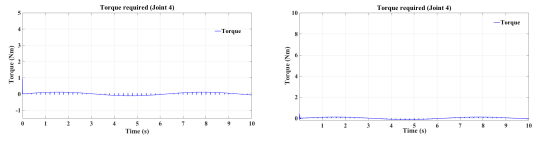

(a) (b)

Fig. 19: The torque required by (Joint 4): (a) PID (b) PD-Fuzzy Controller.

controllers for each joint. Generally, from these figures, the torques required were small. Although, both controllers are able to perform well with such movement, however, based on the deviation and torque analysis, the fuzzy-based PD controller is performing better than the PID controller.

V. Conclusion

In this work, a control mechanism for an upper-limb exoskeleton is presented. There are four important elements in the control mechanism. The elements are the source selection, the joints activation, controller and the plant (upper-limb exoskeleton). In this paper, the source selection was from predefined trajectory. The controller used in this work were PID and fuzzy-based PD controller. The performance of these two controllers were compared in terms of the deviation and torque analysis. Based on the performance shown in this paper, for future, the humanis implemented to ensure the efficiency of the proposed control mechanism.

VI. Acknowledgements

Siti Khadijah Ali is on study leave and supported financially by the Malaysia of Higher Education (MOHE), Universiti Putra Malaysia and University of Sheffield.

References

[1] Seth, D., Chablat, D., Bennis, F., Sakka, S., Jubeau, M., and Nordez, A. (2016). Validation of a new dynamic muscle fatigue model and dmet analysis. The International Journal of Virtual Reality, 2016(16).

[2] Sakka, S., Chablat, D., Ma, R., and Bennis, F. (2015). Predictive model of the human muscle fatigue: application to repetitive pushpull tasks with light external load. International Journal of Human Factors Modelling and Simulation, 5(1), 81-97.

[3] Ma, R., Chablat, D., and Bennis, F. (2013). A new approach to muscle fatigue evaluation for Push/Pull task. In Romansy 19Robot Design, Dynamics and Control (pp. 309-316). Springer, Vienna.

[4] Ma, L., Chablat, D., Bennis, F., and Zhang, W. (2009). A new simple dynamic muscle fatigue model and its validation. International Journal of Industrial Ergonomics, 39(1), 211-220.

[5] Ma, L., Bennis, F., Chablat, D., and Zhang, W. (2008, April). Framework for dynamic evaluation of muscle fatigue in manual handling work. In Industrial Technology, 2008. ICIT 2008. IEEE International Conference on (pp. 1-6). IEEE.

[6] Giat, Y., Mizrahi, J., and Levy, M. (1993). A musculotendon model of the fatigue profiles of paralyzed quadriceps muscle under FES. IEEE transactions on biomedical engineering, 40(7), 664-674.

[7] Liu, J. Z., Brown, R. W., and Yue, G. H. (2002). A dynamical model of muscle activation, fatigue, and recovery. Biophysical journal, 82(5), 2344-2359.

[8] Ma, L., Chablat, D., Bennis, F., Zhang, W., Hu, B., and Guillaume, F. (2011). A novel approach for determining fatigue resistances of different muscle groups in static cases. International Journal of Industrial Ergonomics, 41(1), 10-18.

[9] Ma, L., Chablat, D., Bennis, F., Zhang, W., and Guillaume, F. (2010). A new muscle fatigue and recovery model and its ergonomics application in human simulation. Virtual and Physical Prototyping, 5(3), 123-137.

[10] Ma, R., Chablat, D., Bennis, F., and Ma, L. (2012). Human muscle fatigue model in dynamic motions. In Latest Advances in Robot Kinematics (pp. 349-356). Springer, Dordrecht.

[11] Sakka, S., Chablat, D., Ma, R., and Bennis, F. (2015). Predictive model of the human muscle fatigue: application to repetitive pushpull tasks with light external load. International Journal of Human Factors Modelling and Simulation, 5(1), 81-97.

[12] Gowiski, S., Krzyyski, T., Pecolt, S., and Maciejewski, I. (2015). Design of motion trajectory of an arm exoskeleton. Archive of Applied Mechanics, 85(1), 75-87.

[13] Huang, J., Huo, W., Xu, W., Mohammed, S., and Amirat, Y. (2015). Control of upper-limb power-assist exoskeleton using a human-robot interface based on motion intention recognition. IEEE transactions on automation science and engineering, 12(4), 1257-1270.

[14] Ochoa Luna, C., Habibur Rahman, M., Saad, M., Archambault, P. S., and Bruce Ferrer, S. (2015). Admittance-based upper limb robotic active and active-assistive movements. International Journal of Advanced Robotic Systems, 12(9), 117.

[15] Chen, C. J., Cheng, M. Y., and Su, K. H. (2013, November). Observer-based impedance control and passive velocity control of power assisting devices for exercise and rehabilitation. In Industrial Electronics Society, IECON 2013-39th Annual Conference of the IEEE (pp. 6502-6507). IEEE.

[16] Kiguchi, K. (2007). Active exoskeletons for upper-limb motion assist. International Journal of Humanoid Robotics, 4(03), 607-624.

[17] Kiguchi, K., and Hayashi, Y. (2012). An EMG-based control for an upper-limb power-assist exoskeleton robot. IEEE Transactions on Systems, Man, and Cybernetics, Part B (Cybernetics), 42(4), 1064-1071.

[18] de Looze, M. P., Bosch, T., Krause, F., Stadler, K. S., and OSullivan, L. W. (2016). Exoskeletons for industrial application and their potential effects on physical work load. Ergonomics, 59(5), 671-681.

[19] Rashedi, E., Kim, S., Nussbaum, M. A., and Agnew, M. J. (2014). Ergonomic evaluation of a wearable assistive device for overhead work. Ergonomics, 57(12), 1864-1874.

[20] Beattie, E., McGill, N., Parrotta, N., and Vladimirov, N. (2012). Titan: A Powered, Upper-Body Exoskeleton. Retrieved November, 22, 2014.

[21] Carignan, C., Tang, J., Roderick, S., and Naylor, M. (2007, June). A configuration-space approach to controlling a rehabilitation arm exoskeleton. In Rehabilitation Robotics, 2007. ICORR 2007. IEEE 10th International Conference on (pp. 179-187). IEEE.

[22] Gupta, A., and O'Malley, M. K. (2007). Robotic exoskeletons for upper extremity rehabilitation. In Rehabilitation Robotics. InTech.

[23] Ma, R., Chablat, D., Bennis, F., and Ma, L. (2012). Human muscle fatigue model in dynamic motions. In Latest Advances in Robot Kinematics (pp. 349-356). Springer, Dordrecht.